

Elastography: modality-specific approaches, clinical applications, and research horizons

Yufei Li · Jess G. Snedeker

Received: 11 January 2010 / Revised: 24 February 2010 / Accepted: 24 February 2010 / Published online: 30 March 2010
© ISS 2010

Abstract Manual palpation has been used for centuries to provide a relative indication of tissue health and disease. Engineers have sought to make these assessments increasingly quantitative and accessible within daily clinical practice. Since many of the developed techniques involve image-based quantification of tissue deformation in response to an applied force (i.e., “elastography”), such approaches fall squarely within the domain of the radiologist. While commercial elastography analysis software is becoming increasingly available for clinical use, the internal workings of these packages often remain a “black box,” with limited guidance on how to usefully apply the methods toward a meaningful diagnosis. The purpose of the present review article is to introduce some important approaches to elastography that have been developed for the most widely used clinical imaging modalities (e.g., ultrasound, MRI), to provide a basic sense of the underlying physical principles, and to discuss both current and potential (musculoskeletal) applications. The article also seeks to provide a perspective on emerging approaches that are rapidly developing in the research laboratory (e.g., optical coherence tomography, fibered confocal microscopy), and which may eventually gain a clinical foothold.

Keywords Elastography · Elasticity imaging · Sonoelastography · Magnetic resonance elastography · Optical elastography · Musculoskeletal tissue imaging

Introduction

Changes in tissue mechanical properties are a well established marker of certain diseases. For example, physicians have been using palpation to detect breast and prostate tumors for centuries. This is based on the fact that tumor tissues often have a much higher compressive stiffness than normal ones [1]. In orthopedics, reduced compressive stiffness has been reported to be an early indication of cartilage degeneration [2]. Injured and diseased tendon will also exhibit aberrant biomechanical properties (e.g., stiffness, failure load) and healing tendon will progressively regain its stiffness [3]. Osteoporotic bones have lower stiffness and strength, making them more susceptible to fracture [4]. In short, a way of measuring the mechanical properties of tissue can be helpful for clinical diagnosis of existing pathologies, tracking of healing progress, or for prediction of injury risk and prognosis for the likelihood of healing.

Manual palpation is a common, albeit subjective, measure of tissue mechanical properties for diagnostic purposes. It nonetheless shares a basic operating principle with more sophisticated approaches that apply an external load to a tissue while measuring consequent tissue deformation. Recent advancements in imaging techniques have opened possibilities for accurately measuring these deformations in vivo and later extracting functional/biomechanical properties. Ophir et al. [5] first used the term “elastography” to describe the method of quantitative imaging of the distribution of biological tissue strains (a measure of tissue stretch that is normalized to

Y. Li · J. G. Snedeker (✉)
Department of Orthopaedics, University Hospital Balgrist,
Forchstrasse 340,
8008 Zurich, Switzerland
e-mail: jsnedeker@research.balgrist.ch

Y. Li · J. G. Snedeker
Department of Mechanical Engineering, ETH Zurich,
Wolfgang-Pauli-Strasse 10,
8093 Zurich, Switzerland

the dimensions of the undeformed tissue) and elastic modulus (a material property that describes relative tissue compliance). Ultrasound and magnetic resonance imaging were the earliest adapted modalities used for elastography and such approaches have evolved over many years. The current perspective article seeks to review newer techniques and applications that have emerged in the past 5 years using ultrasound and magnetic resonance elastography as well as other imaging modalities. The goal is to thus provide an overview of elastography methods developed for common clinical imaging modalities and their present and potential clinical applications.

Mechanical properties of tissue

Reflecting their composition, most tissues in the human body are viscoelastic, possessing the properties of both elastic (solid) and viscous (fluid-like) materials. The response of a tissue to an applied load (stress–strain curves as in Fig. 1) will vary depending on the relative elastic and viscoelastic properties of a tissue. While the viscous properties are closely related to function in some cases (such as dissipation of impact energy), in this review we will focus on the elastic properties of tissue, which are most often described by elastic modulus.

Most biological tissues are structurally complex, with accordingly complex material behaviors that complicate analytical treatment. For the purposes of conceptual (mathematical) expedience, engineers often describe material behavior in terms of a few parameters that approximately characterize a substance's tendency to deform under applied stress. Elastic modulus is most commonly used, and is defined as the slope of the stress–strain curve (how much the material stretches in response to an incremental change

in applied stress). The precise definition of elastic modulus depends on how stress and strain are described. The most common definitions are Young's modulus (E), shear modulus (G), and bulk modulus (K). Young's modulus is defined as tensile (or compressive) stress over tensile (or compressive) strain, while shear modulus is defined as shear stress over shear strain. Bulk modulus is an extension of Young's modulus in three dimensions and is defined as volumetric stress over volumetric strain. The Poisson's ratio (ν) is also a commonly used parameter in biomechanics. It is defined as the ratio of transverse strain over axial strain when a sample is stretched. The relationship among E , G , K , and ν can be described by:

$$G = \frac{E}{2(1 + \nu)} \quad (1)$$

and,

$$K = \frac{E}{3(1 - 2\nu)} \quad (2)$$

Given their high water content, most soft tissues inside the human body are nearly incompressible, which means they have a Poisson ratio close to 0.5. This gives a simplified relationship between shear modulus (G) and Young's modulus (E) of $E \approx 3G$. Since the bulk modulus does not vary much (less than 15%) for human tissues, shear modulus and Young's modulus are the most suitable parameters to measure.

Young's modulus and shear modulus are terms that describe "material quality," and are constructed to be independent of the shape or size of the tissue. This makes comparison among different tissues possible. When one is less directly concerned with the tissue, but rather with the functional anatomical unit (e.g., the Achilles tendon) itself, "structural properties" are usually described. For instance, the engineering term "stiffness" is defined as the ratio of the applied force on a structure over the length change induced by that force. While structural "stiffness" and material "modulus" are related, they have distinct biomechanical meanings with regard to the dimension of the tissues being considered.

Imaging modalities

Almost all elastography approaches involve some method of tissue excitation to apply mechanical stress to a region of interest, then use imaging methods to measure the displacement prior to and immediately following the applied stress. Several imaging modalities have been employed to measure these displacements. In this regard, ultrasound and MR elastography have been under very active development for the past 20 years. They infer displacements using ultra-

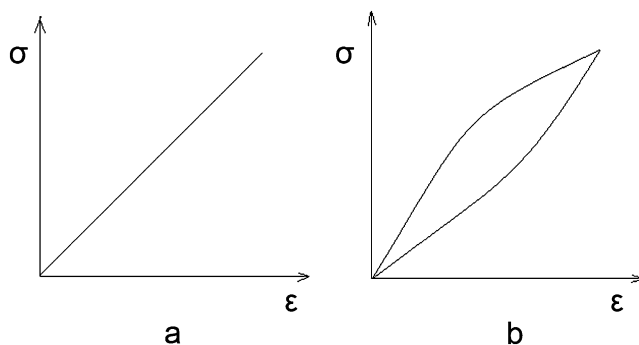


Fig. 1 Stress vs strain curves for **a** purely elastic material and **b** a viscoelastic material. The viscous nature of biological materials dissipates energy as a tissue is loaded and unloaded, as reflected in the non-linear loop of the material curve. More elastic tissues (like tendon) behave like a spring, loading and unloading with minimal energy loss. Highly viscoelastic tissues like cartilage have inherent dissipative properties that are useful for absorbing shock

sound or MR signals directly, or by tracking changes in the distance between anatomical landmarks. With recent advancements in image registration, feature tracking and computational power, displacements can now be obtained by comparing pre- and post-stress images using many other imaging modalities, often in real-time. The following sections of the paper will address these imaging modalities separately.

Ultrasound elastography

Ultrasound elastography was the first and most widely researched method. Various approaches to ultrasound elastography have been proposed over the years. According to tissue excitation and displacement detection methods, they can be further classified into four subcategories: compression elastography, sonoelastography, transient elastography, and acoustic radiation force elastography.

Compression elastography

Compression elastography, also known as the static method or quasi-static method, refers to lower frequency (less than 10 Hz) compressions during tissue excitation. It is normally performed using manual manipulation or sometimes even relying on natural internal movements, such as respiration, heartbeat, etc. The study of ultrasound elasticity imaging began with Dickinson and Hill [6] and Wilson and Robinson [7]. They used the correlation between successive A-scans and M-scans respectively to measure low velocity motions in liver tissues caused by aortic pulsation. Displacement was calculated from the time integral of velocity. This method had been further extended to two dimensions with the advancement of ultrasound technology [8, 9]. In 1991, Ophir et al. [5] applied external compression to measure the resultant strain field and first referred to the method as elastography. It was assumed that the applied stress was uniform. Thus, the derived elastic moduli were inversely proportional to the measured strain (higher modulus tissues were indicated by less tissue stretch). Here, the term “elastogram” was coined to describe the resultant elastic modulus distribution. For visualization purposes, elastograms are often color-coded so that lesions with different elastic moduli can be clearly identified. This method has been developed, with oversampling (quasistatic cyclic compression) to improve signal to noise and help eliminate artifacts [10].

Compression elastography has been shown to be helpful in breast and prostate tumor detection [11, 12], thyroid tumor diagnosis [13], intravascular plaque characterization [14], and assessment of tendinosis [15–18], among other clinical applications.

Sonoelastography

In 1987, Krouskop et al. [19] proposed a one-dimensional (1-D) method to measure the mechanical properties of soft tissue at desired points. External low frequency (10 Hz) vibrations were applied to the tissue and wave velocity was measured using a gated Doppler ultrasound motion sensing system. Yamakoshi et al. [20] used higher frequency (several hundred Hertz) vibrations in a similar manner. Both the amplitude and phase of internal vibration were measured from Doppler frequency modulation of simultaneously transmitted probing ultrasound waves.

The first actual image of an elastic modulus using this approach was created by Lerner et al. [21], who introduced the term “sonoelasticity imaging.” This method was further developed by Parker et al. [22–25] and has subsequently been referred to as “sonoelastography.” Here, Doppler shift was used to detect the shear velocity of soft tissues induced by external vibrations. Then, Young’s modulus (E) could be calculated as a function of shear velocity (C_s) and material density (ρ) by:

$$E = 3\rho C_s^2 \quad (3)$$

Another shear wave source was added to the system so that the pattern of interference between the two waves could be imaged and correlated with shear velocity in the medium (Fig. 2). This approach slowed the resultant shear wave such that a commercially available ultrasound system could be used for imaging [26–28]. Three-dimensional sonoelastography was developed by acquiring a sequence (“stack”) of 2D images then registering them to form a volume [29–31].

Sonoelastography has been mainly applied in prostate tumor detection [28, 29, 32] and liver disease [33], among other applications.

Transient elastography

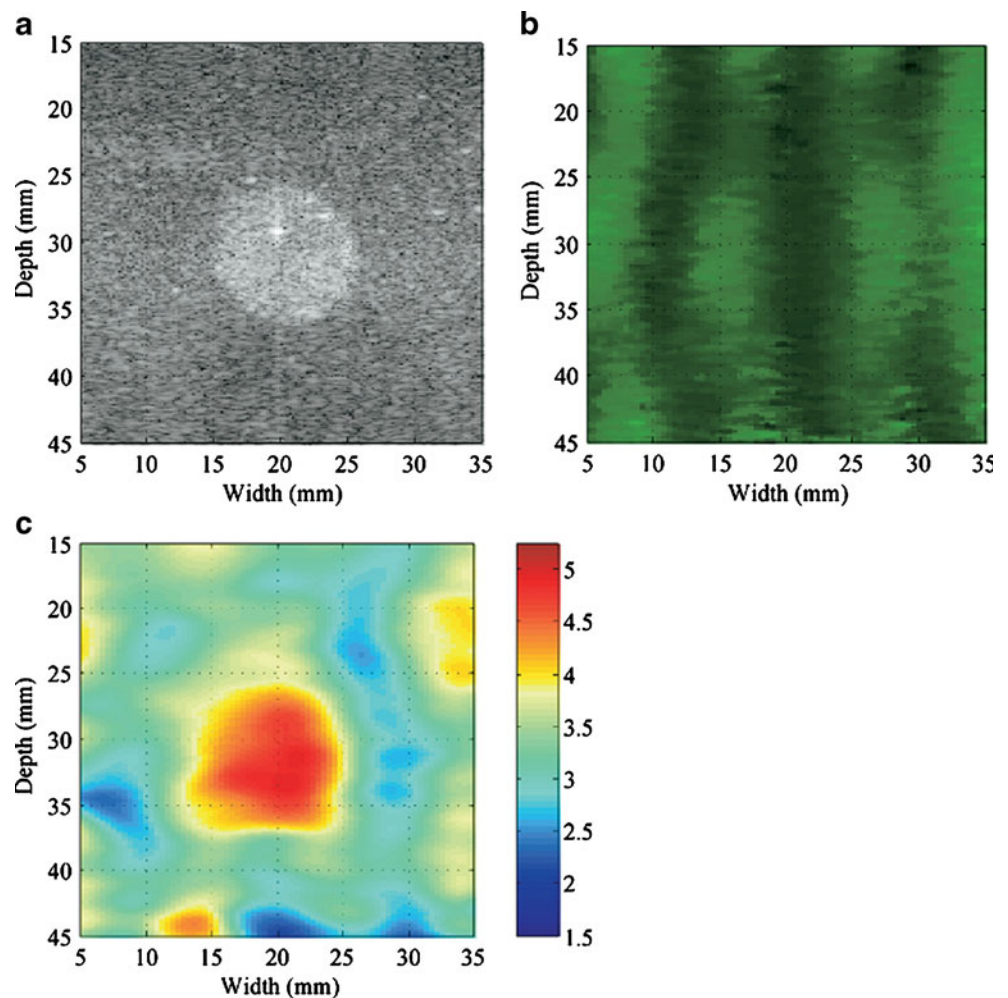
One of the drawbacks of sonoelastography is a bias related to reflected waves created at tissue boundaries. To avoid this problem, transient elastography was proposed. The method utilized a short tone burst of vibration so that forward propagating waves could be separated from reflected waves using a pulse-echo system [34, 35].

Transient elastography has shown great promise for the detection of liver disease, especially fibrosis [36]. Other applications include breast tumor detection [37] and muscle stiffness measurement [38, 39].

Acoustic radiation force elastography

In contrast to all the above-described methods by which tissues are excited externally, acoustic radiation force

Fig. 2 Results reprinted from Hoyt et al. [24]. The images represent sonoelastographic techniques applied to a phantom intended to mimick heterogeneous tissue (13×13×8 cm) containing a 1 cm diameter stiff circular inclusion. Results depict the matched **a** B-mode ultrasound image, **b** sonoelastogram and **c** shear velocity images (units m/s)



elastography uses internal tissue excitation through a focused ultrasound pulse [40–42]. The force induced by the pulse can be calculated according to:

$$F = 2\alpha I/c \quad (4)$$

where α is the absorption coefficient of the medium, c is the speed of sound in the propagation medium, and I is the intensity of the acoustic beam [42]. After excitation, displacements can be measured using pulse echo techniques with normal pulses at a diagnostic level.

Acoustic radiation force elastography has been applied to breast lesion imaging [43], abdominal imaging [44], as well as providing guidance for cardiac and liver tissue ablation [45, 46].

Magnetic resonance elastography

Compared with ultrasound imaging, magnetic resonance imaging (MRI) offers advantages for elastographic imaging in terms of a larger field of view and the potential to more

easily incorporate a three-dimensional analysis. Muthupillai et al. [47] proposed the magnetic resonance elastography (MRE) method using phase-sensitive magnetic resonance to measure shear modulus. The tissue excitation method was similar to that of sonoelastography by which high-frequency (200 to 400 Hz) vibrations were applied externally to the tissue surface to induce shear waves within the tissue. Tissue displacements were then correlated with the phase shifts of the magnetic resonance signals (e.g., Fig. 3) [47–49]. Various data processing techniques have been proposed to relate these displacements to mechanical properties. More comprehensive summaries of this technique can be found elsewhere [50].

It has been reported that several factors can affect results obtained using MRE including the frequency of tissue excitation, tissue temperature, and the direction of wave propagation and polarization [51]. While these factors do influence quantitative measurements, relative assessments based on qualitative tissue stiffness measurements in applications like tumor lesion detection are less sensitive.

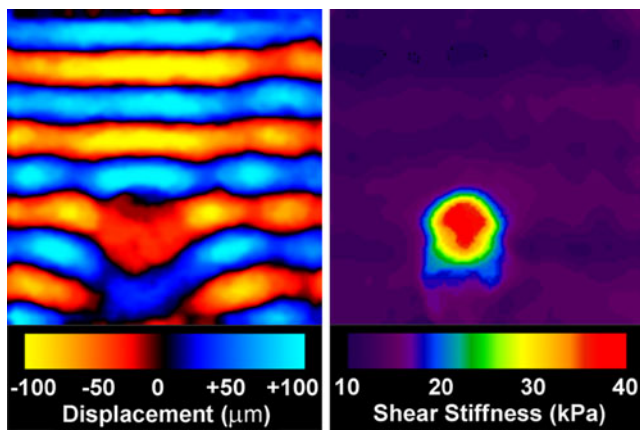


Fig. 3 Magnetic resonance elastogram showing the typical spatial resolution and measurable tissue stiffness range achievable with a clinical grade MRI. **a** Shear waves propagating in a homogeneous phantom with an embedded 1.5 cm diameter cylinder of stiffer gel. **b** The elastogram depiction of the object. Reprinted with permission from Manduca et al. [50]

Magnetic resonance elastography has been used in a wide variety of applications spanning breast cancer detection [52], liver disease detection [53], brain tissue stiffness measurement [54], lung mechanical properties measurement [55], and muscle tissue characterization [56–58].

Optical elastography

Optical elastography (e.g., clinical endoscopy) is also a well-established concept that has many methodological forms. White light elastography has been used to replace strain gauges in the measurement of tissue mechanical properties in the laboratory [59]. Because of the limited penetration of white light, in vivo application of white light elastography has been mainly limited to skin disease detection [60]. We describe below two other forms of optical elastography that have been developed in recent years that take advantage of advancements in optical imaging.

Optical coherence tomography (OCT) is a relatively new optical imaging modality for imaging internal tissue structures [61]. It is similar to ultrasound imaging except that it uses infrared light waves instead of acoustic waves. OCT allows tissue imaging at a microscopic level (spatial resolutions around 10 μm) and it is relatively inexpensive and portable [62]. OCT elastography was proposed to image micrometer-level displacements and strain distributions induced by compression in 1998 [63]. The tissue excitation method used in this case was a small step-wise increase in compressive force on external tissue surfaces. The displacements were tracked using speckle tracking algorithms, and tissue strain maps were then calculated. In this modality, feature tracking in the images is of utmost importance, and various tracking algorithms have been

compared for performance and accuracy [64–66]. Clinically, OCT has been mainly applied on extracardiac arteries and veins for coronary disease detection [67]. Other applications include quantification of the mechanical properties of developing tissues [68] and imaging of the stiffness of skin lesions [69].

In 2004, fibered confocal fluorescence microscopy (FCFM) was first described [70]. FCFM combines the advantages of a confocal microscope and endoscope to allow in vivo measurement of targeted tissues at the tissue and cell levels. The technique was later applied to measure soft tissue material properties in vivo using fluorescently labeled cell nuclei as markers of tissue displacement [71–73]. The method has been shown to be able to detect very small mechanical tissue defects, while simultaneously monitoring the key biological aspects of cell behaviors.

Improved elastogram analysis using the inverse finite element method

The finite element method (FEM) has been used in the medical field to predict tissue deformations (for instance related to injury and failure) given the anatomy, mechanical properties, and applied loads. If the tissue deformations are already known (e.g. from the clinical imaging data of a mechanically loaded tissue), finite element methods can be used in an “inverse” approach to extract the tissue mechanical properties. Here, the geometry and deformation are obtained by taking images before and after deformation. A finite element model is then reconstructed from the images and material properties are obtained by iteratively adjusting the parameters in the model until the predicted strains most closely match the measured strains. Such an approach is being increasingly used, and offers great potential for improved extraction of functional biomechanical information from clinical imaging data [74]. For elastography methods that only provide relative measures of tissue stiffness because of difficulties in accurately measuring local strain distributions, inverse FEM can be used as a supplementary method to quantitatively derive material properties [75].

An advantage of inverse FEM is that it is modality-independent. Images from all modalities can be applied as long as they provide enough data for model construction and deformation calculation. Miga et al. [76, 77] helped pioneer this approach and have coined it “modality-independent elastography.” This flexibility with regard to imaging modality has resulted in its use in a wide range of clinical applications including cardiovascular diseases [74], mammography [77], dermoscopy [76], atherosclerotic coronary plaques [78], myometrium modeling [79], and liver hemangioma [75].

Application to musculoskeletal tissues

While the primary clinical application of elastography remains for tumor detection, its potential application to musculoskeletal tissues has increasingly driven research activity around the development of new approaches and the translation of existing approaches to clinical devices. Until now, the most plausible clinical application of functional imaging of skeletal tissues has been with regard to the early diagnosis of tissue and joint degeneration [80], and the assessment of osteoporosis-related fracture risk [81, 82]. Also possible, but less developed, is the potential for imaging-based assessment of healing, and the use of this information in modulating a particular therapy (or rehabilitative protocol) based on functional readouts.

Muscle is the mostly widely researched musculoskeletal tissue for elastography. Dresner et al. [56] demonstrated the applicability of MR elastography to measure skeletal muscle stiffness. The same method has been applied to quantify differences in muscle stiffness between normal and dysfunctional (lower-extremity neuromuscular dysfunction) groups [83] and for identifying taut bands with higher stiffness than normal muscles [84]. Bensamoun et al. [85, 86] quantitatively measured the stiffness of thigh muscle and compared the results before and after treatment for hyperthyroid activity. MR elastography measurements of skeletal muscles have been verified against mathematical models and correlated with electromyographic data [87]. The effects of aging on muscle stiffness have been examined by MRE [88]. As a competing method, sono-elastography has also been applied to measure skeletal muscle elasticity [89–91].

Assessing joint tissue mechanics presents another potentially important application of elastography. MR elastography has been applied to measure cartilage deformation in an attempt to link mechanics to disease [92–94]. Tendon and ligament strain measurements have been performed by ultrasound elastography (Fig. 4) [17, 95, 96], and the sensitivity, specificity, accuracy, and reproducibility of the method have been explored in the imaging of symptomatic Achilles tendons [15, 17, 18] and for the detection of lateral epicondylitis [16]. Optical methods with fibered confocal fluorescence microscopy have also been developed for relating tendon stretch to tissue health [71–73]. A recent review of ultrasound elastography for musculoskeletal applications can be found by Klauser and Peetrons [97].

Conclusion and future outlook

Elastography provides a non-invasive way to measure tissue mechanical properties in vivo. It provides additional

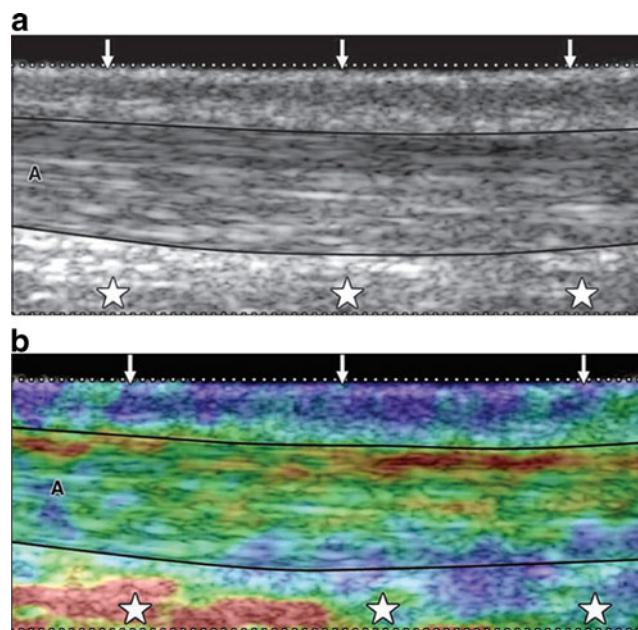


Fig. 4 Application of ultrasound elastography for the diagnosis of Achilles tendinopathy. **a** The tendon is located between *lines*, *arrows* indicate the skin, and *stars* show anterior peritendinous tissue. **b** Real-time sonoelastography image corresponding to **a** shows changes in tissue elasticity. Distinct softening can be seen in the dorsal part of the Achilles tendon. *Red* represents soft tissue; *blue and green*, hard tissue; and *yellow*, tissues of intermediate stiffness. Reprinted with permission from De Zordo et al. [17]

functional information that cannot otherwise be seen using traditional imaging methods. Its application has been expanding rapidly over the past few years. New methods for different clinical applications are emerging, but need to be carefully characterized before meaningful clinical application is possible.

The available methods each have their own merits and drawbacks. For example, ultrasound elastography has the benefits of low cost and short acquisition time, but suffers from generally poor spatial resolution (e.g., compression elastography has a spatial resolution of 1.5 mm at its theoretical limit [98]). MRE has a better potential resolution (35 μm at an extremely high magnetic field of 11.7 T [99]) and a larger field of view with a capacity for 3D measurement, but it is relatively more expensive and long acquisition times complicate the acquisition of images of loaded tissues. Optical elastography has very good resolution (5–10 μm [62, 72]), but a limited field of view and depth of tissue penetration. Most of the post-processing methods used to extract meaningful functional information (such as inverse FEM) are far from automatic and may require specialized computational infrastructure. In any case, the method, or even a combination of several methods, that is most suitable will depend on the underlying pathology, clinical utility, and cost–benefit of the assessment.

Several steps are required for a new method to progress from the laboratory to the bedside, including system development, feasibility testing, limited trials, and multi-center trials before eventually becoming commercialization and implementation within a standard of care [100]. Only ultrasound elastography is commercially available at the moment. Siemens (Munich, Germany) offers two elastography platforms: eSie Touch™ (compression elastography) and Virtual Touch™ (acoustic radiation force elastography) for their ultrasound systems. Hitachi (Tokyo, Japan) includes an E-mode for elastography measurement in their HI VISION™ 900 system. SuperSonic (SuperSonic Imagine, Aix-en-Provence, France) produces machines equipped with ShearWave™ elastography (acoustic radiation force elastography) for quantitative tissue elasticity measurements. Fibroscan (Echosens, Paris, France) uses transient elastography designed specifically for measuring the degree of liver fibrosis. Most other elastography modalities are still in pilot studies or clinical trials, but it is to be expected that additional commercial products will become increasingly available in the near future.

References

- Krouskop TA, Wheeler TM, Kallel F, Garra BS, Hall T. Elastic moduli of breast and prostate tissues under compression. *Ultrasound Imaging*. 1998;20(4):260–74.
- Franz T, Hasler EM, Hagg R, Weiler C, Jakob RP, Mainil-Varlet P. In situ compressive stiffness, biochemical composition, and structural integrity of articular cartilage of the human knee joint. *Osteoarthritis Cartilage*. 2001;9(6):582–92.
- Steiner M. Biomechanics of tendon healing. *J Biomech*. 1982;15(12):951–8.
- Dickenson RP, Hutton WC, Stott JR. The mechanical properties of bone in osteoporosis. *J Bone Joint Surg Br*. 1981;63-B(2):233–8.
- Ophir J, Cespedes I, Ponnekanti H, Yazdi Y, Li X. Elastography: a quantitative method for imaging the elasticity of biological tissues. *Ultrasound Imaging*. 1991;13(2):111–34.
- Dickinson RJ, Hill CR. Measurement of soft-tissue motion using correlation between A-scans. *Ultrasound Med Biol*. 1982;8(3):263–71.
- Wilson LS, Robinson DE. Ultrasonic measurement of small displacements and deformations of tissue. *Ultrasound Imaging*. 1982;4(1):71–82.
- Bjaerum S, Torp H, Kristoffersen K. Clutter filters adapted to tissue motion in ultrasound color flow imaging. *IEEE Trans Ultrason Ferroelectr Freq Control*. 2002;49(6):693–704.
- Mai JJ, Insana MF. Strain imaging of internal deformation. *Ultrasound Med Biol*. 2002;28(11–12):1475–84.
- O'Donnell M, Skovoroda AR, Shapo BM, Emelianov SY. Internal displacement and strain imaging using ultrasonic speckle tracking. *IEEE Trans Ultrason Ferroelectr Freq Control*. 1994;41(3):314–25.
- Garra BS, Cespedes EI, Ophir J, Spratt SR, Zurbier RA, Magnant CM, et al. Elastography of breast lesions: initial clinical results. *Radiology*. 1997;202(1):79–86.
- Lorenz A, Sommerfeld HJ, Garcia-Schurmann M, Philippou S, Senge T, Ermert H. A new system for the acquisition of ultrasonic multicompression strain images of the human prostate in vivo. *IEEE Trans Ultrason Ferroelectr Freq Control*. 1999;46(5):1147–54.
- Bae U, Dighe M, Dubinsky T, Minoshima S, Shamdasani V, Kim Y. Ultrasound thyroid elastography using carotid artery pulsation: preliminary study. *J Ultrasound Med*. 2007;26(6):797–805.
- De Korte CL, Pasterkamp G, van der Steen AFW, Woutman HA, Bom N. Characterization of plaque components with intravascular ultrasound elastography in human femoral and coronary arteries in vitro. *Circulation*. 2000;102(6):617–23.
- Drakonaki EE, Allen GM, Wilson DJ. Real-time ultrasound elastography of the normal Achilles tendon: reproducibility and pattern description. *Clin Radiol*. 2009;64(12):1196–202.
- De Zordo T, Lill SR, Fink C, Feuchtner GM, Jaschke W, Bellmann-Weiler R, et al. Real-time sonoelastography of lateral epicondylitis: comparison of findings between patients and healthy volunteers. *AJR Am J Roentgenol*. 2009;193(1):180–5.
- De Zordo T, Fink C, Feuchtner GM, Smekal V, Reindl M, Klauser AS. Real-time sonoelastography findings in healthy Achilles tendons. *AJR Am J Roentgenol*. 2009;193(2):W134–8.
- De Zordo T, Chhem R, Smekal V, Feuchtner G, Reindl M, Fink C, et al. Real-time sonoelastography: findings in patients with symptomatic Achilles tendons and comparison to healthy volunteers. *Ultraschall Med*. 2009; doi:10.1055/s-0028-1109809.
- Krouskop TA, Dougherty DR, Vinson FS. A pulsed Doppler ultrasonic system for making noninvasive measurements of the mechanical properties of soft tissue. *J Rehabil Res Dev*. 1987;24(2):1–8.
- Yamakoshi Y, Sato J, Sato T. Ultrasonic imaging of internal vibration of soft tissue under forced vibration. *IEEE Trans Ultrason Ferroelectr Freq Control*. 1990;37(2):45–53.
- Lerner RM, Parker KJ, Holen J, Gramiak R, Waag RC. Sonoelasticity: medical elasticity images derived from ultrasound signals in mechanically vibrated targets. *Proceedings of the 16th International Acoustical Imaging Symposium*. New York: Plenum; 1988;317–27.
- Parker KJ, Fu D, Graceswki SM, Yeung F, Levinson SF. Vibration sonoelastography and the detectability of lesions. *Ultrasound Med Biol*. 1998;24(9):1437–47.
- Parker KJ, Huang SR, Musulin RA, Lerner RM. Tissue response to mechanical vibrations for "sonoelasticity imaging". *Ultrasound Med Biol*. 1990;16(3):241–6.
- Hoyt K, Parker KJ, Rubens DJ. Real-time shear velocity imaging using sonoelastographic techniques. *Ultrasound Med Biol*. 2007;33(7):1086–97.
- Lerner RM, Huang SR, Parker KJ. "Sonoelasticity" images derived from ultrasound signals in mechanically vibrated tissues. *Ultrasound Med Biol*. 1990;16(3):231–9.
- Hoyt K, Castaneda B, Parker KJ. Two-dimensional sonoelastographic shear velocity imaging. *Ultrasound Med Biol*. 2008;34(2):276–88.
- Wu Z, Hoyt K, Rubens DJ, Parker KJ. Sonoelastographic imaging of interference patterns for estimation of shear velocity distribution in biomaterials. *J Acoust Soc Am*. 2006;120(1):535–45.
- Hoyt K, Parker KJ, Rubens DJ. P2E-7 Sonoelastographic shear velocity imaging: experiments on tissue phantom and prostate. *Ultrasonics Symposium, 2006 IEEE*; 2006;1686–9.
- Taylor LS, Porter BC, Nadasdy G, di Sant'Agnese PA, Pasternack D, Wu Z, et al. Three-dimensional registration of prostate images from histology and ultrasound. *Ultrasound Med Biol*. 2004;30(2):161–8.

30. Wu Z, Taylor LS, Rubens DJ, Parker KJ. Shear wave focusing for three-dimensional sonoelastography. *J Acoust Soc Am*. 2002;111(1 Pt 1):439–46.
31. Taylor LS, Porter BC, Rubens DJ, Parker KJ. Three-dimensional sonoelastography: principles and practices. *Phys Med Biol*. 2000;45(6):1477–94.
32. Hoyt K, Castaneda B, Zhang M, Nigwekar P, di Sant'agnese PA, Joseph JV, et al. Tissue elasticity properties as biomarkers for prostate cancer. *Cancer Biomarkers*. 2008;4(4–5):213–25.
33. Carstensen EL, Parker KJ, Lerner RM. Elastography in the management of liver disease. *Ultrasound Med Biol*. 2008;34(10):1535–46.
34. Sandrin L, Catheline S, Tanter M, Fink M. 2D Transient elastography. 2001;485–92.
35. Catheline S, Wu F, Fink M. A solution to diffraction biases in sonoelasticity: the acoustic impulse technique. *J Acoust Soc Am*. 1999;105(5):2941–50.
36. Sandrin L, Fourquet B, Hasquenoph JM, Yon S, Fournier C, Mal F, et al. Transient elastography: a new noninvasive method for assessment of hepatic fibrosis. *Ultrasound Med Biol*. 2003;29(12):1705–13.
37. Bercoff J, Chaffai S, Tanter M, Sandrin L, Catheline S, Fink M, et al. In vivo breast tumor detection using transient elastography. *Ultrasound Med Biol*. 2003;29(10):1387–96.
38. Sabra KG, Conti S, Roux P, Kuperman WA. Passive in vivo elastography from skeletal muscle noise. *Appl Phys Lett*. 2007;90(19):194101–3.
39. Nordez A, Gennisson JL, Casari P, Catheline S, Cornu C. Characterization of muscle belly elastic properties during passive stretching using transient elastography. *J Biomech*. 2008;41(10):2305–11.
40. Fahey BJ, Nightingale KR, Nelson RC, Palmeri ML, Trahey GE. Acoustic radiation force impulse imaging of the abdomen: demonstration of feasibility and utility. *Ultrasound Med Biol*. 2005;31(9):1185–98.
41. Nightingale K, Soo MS, Palmeri M, Congdon A, Frinkley K, Trahey G. Imaging tissue mechanical properties using impulsive acoustic radiation force. *Biomedical Imaging: Nano to Macro, 2004 IEEE International Symposium*; 2004;41–4.
42. Nightingale K, Soo MS, Nightingale R, Trahey G. Acoustic radiation force impulse imaging: in vivo demonstration of clinical feasibility. *Ultrasound Med Biol*. 2002;28(2):227–35.
43. Sharma AC, Soo MS, Trahey GE, Nightingale KR. Acoustic radiation force impulse imaging of in vivo breast masses. *Ultrasonics Symposium, 2004 IEEE*. 2004;728–31.
44. Fahey BJ, Nelson RC, Hsu SJ, Bradway DP, Dumont DM, Trahey GE. In vivo guidance and assessment of liver radio-frequency ablation with acoustic radiation force elastography. *Ultrasound Med Biol*. 2008;34(10):1590–603.
45. Hsu SJ, Bouchard RR, Dumont DM, Wolf PD, Trahey GE. In vivo assessment of myocardial stiffness with acoustic radiation force impulse imaging. *Ultrasound Med Biol*. 2007;33(11):1706–19.
46. Nightingale K, Fahey B, Hsu S, Frinkley K, Dahl J, Palmeri M, et al. On the potential for guidance of ablation therapy using acoustic radiation force impulse imaging. *4th IEEE International Symposium on Biomedical Imaging: From Nano to Macro, 2007 ISBI*. 2007;1116–9.
47. Muthupillai R, Lomas DJ, Rossman PJ, Greenleaf JF, Manduca A, Ehman RL. Magnetic resonance elastography by direct visualization of propagating acoustic strain waves. *Science*. 1995;269(5232):1854–7.
48. Manduca A, Muthupillai R, Rossman PJ, Greenleaf JF, Ehman RL. Image processing for magnetic-resonance elastography. In: Loew MH, Hanson KM, editors. Newport Beach, CA, USA: SPIE. 1996;616–23.
49. Muthupillai R, Rossman PJ, Lomas DJ, Greenleaf JF, Riederer SJ, Ehman RL. Magnetic resonance imaging of transverse acoustic strain waves. *Magn Reson Med*. 1996;36(2):266–74.
50. Manduca A, Oliphant TE, Dresner MA, Mahowald JL, Kruse SA, Amromin E, et al. Magnetic resonance elastography: non-invasive mapping of tissue elasticity. *Med Image Anal*. 2001;5(4):237–54.
51. Kruse SA, Smith JA, Lawrence AJ, Dresner MA, Manduca A, Greenleaf JF, et al. Tissue characterization using magnetic resonance elastography: preliminary results. *Phys Med Biol*. 2000;45(6):1579–90.
52. McKnight AL, Kugel JL, Rossman PJ, Manduca A, Hartmann LC, Ehman RL. MR elastography of breast cancer: preliminary results. *AJR Am J Roentgenol*. 2002;178(6):1411–7.
53. Huwart L, Peeters F, Sinkus R, Annet L, Salameh N, ter Beek LC, et al. Liver fibrosis: non-invasive assessment with MR elastography. *NMR Biomed*. 2006;19(2):173–9.
54. Xu L, Lin Y, Xi ZN, Shen H, Gao PY. Magnetic resonance elastography of the human brain: a preliminary study. *Acta Radiol*. 2007;48(1):112–5.
55. McGee KP, Hubmayr RD, Levin D, Ehman RL. Feasibility of quantifying the mechanical properties of lung parenchyma in a small-animal model using (1)H magnetic resonance elastography (MRE). *J Magn Reson Imaging*. 2009;29(4):838–45.
56. Dresner MA, Rose GH, Rossman PJ, Muthupillai R, Manduca A, Ehman RL. Magnetic resonance elastography of skeletal muscle. *J Magn Reson Imaging*. 2001;13(2):269–76.
57. Sack I, Bernarding J, Braun J. Analysis of wave patterns in MR elastography of skeletal muscle using coupled harmonic oscillator simulations. *Magn Reson Imaging*. 2002;20(1):95–104.
58. Uffmann K, Maderwald S, Ajaj W, Galban CG, Mateiescu S, Quick HH, et al. In vivo elasticity measurements of extremity skeletal muscle with MR elastography. *NMR Biomed*. 2004;17(4):181–90.
59. Rigozzi S, Muller R, Snedeker JG. Local strain measurement reveals a varied regional dependence of tensile tendon mechanics on glycosaminoglycan content. *J Biomech*. 2009;42(10):1547–52.
60. Zhang Y, Brodell RT, Mostow EN, Vinyard CJ, Marie H. In vivo skin elastography with high-definition optical videos. *Skin Res Technol*. 2009;15(3):271–82.
61. Huang D, Swanson EA, Lin CP, Schuman JS, Stinson WG, Chang W, et al. Optical coherence tomography. *Science*. 1991;254(5035):1178–81.
62. Tearney GJ, Brezinski ME, Bouma BE, Boppart SA, Pitris C, Southern JF, et al. In vivo endoscopic optical biopsy with optical coherence tomography. *Science*. 1997;276(5321):2037–9.
63. Schmitt J. OCT elastography: imaging microscopic deformation and strain of tissue. *Opt Express*. 1998;3(6):199–211.
64. Duncan D, Kirkpatrick S. Performance analysis of a maximum-likelihood speckle motion estimator. *Opt Express*. 2002;10(18):927–41.
65. Kirkpatrick SJ. Optical elastography. In: Valery VT, editor. SPIE. 2001;58–68.
66. Duncan DD, Kirkpatrick SJ. Processing algorithms for tracking speckle shifts in optical elastography of biological tissues. *J Biomed Opt*. 2001;6(4):418–26.
67. Rogowska J, Patel N, Plummer S, Brezinski ME. Quantitative optical coherence tomographic elastography: method for assessing arterial mechanical properties. *Br J Radiol*. 2006;79(945):707–11.
68. Ko HJ, Tan W, Stack R, Boppart SA. Optical coherence elastography of engineered and developing tissue. *Tissue Eng*. 2006;12(1):63–73.
69. Kirkpatrick SJ, Wang RK, Duncan DD, Kulesz-Martin M, Lee K. Imaging the mechanical stiffness of skin lesions by in vivo acousto-optical elastography. *Opt Express*. 2006;14(21):9770–9.

70. Le Goualher G, Perchant A, Genet M, Cavé C, Viellerobe B, Berier F, et al. Towards optical biopsies with an integrated fibered confocal fluorescence microscope. 2004;761–8.
71. Snedeker JG, Arav AB, Zilberman Y, Pelled G, Gazit D. Functional fibered confocal microscopy: a promising tool for assessing tendon regeneration. *Tissue Eng Part C Methods*. 2009;15:485–91.
72. Snedeker JG, Pelled G, Zilberman Y, Ben Arav A, Huber E, Muller R, et al. An analytical model for elucidating tendon tissue structure and biomechanical function from in vivo cellular confocal microscopy images. *Cells Tissues Organs*. 2009;190:111–9.
73. Snedeker JG, Pelled G, Zilberman Y, Gerhard F, Muller R, Gazit D. Endoscopic cellular microscopy for in vivo biomechanical assessment of tendon function. *J Biomed Opt*. 2006;11(6):064010.
74. Moulton MJ, Creswell LL, Actis RL, Myers KW, Vannier MW, Szabo BA, et al. An inverse approach to determining myocardial material properties. *J Biomech*. 1995;28(8):935–48.
75. Aglyamov S, Skovoroda A, Xie H, Kim K, Rubin JM, O'Donnell M, et al. Model-based reconstructive elasticity imaging using ultrasound. *Int J Biomed Imaging*. 2007;2007:35830.
76. Miga MI, Rothney MP, Ou JJ. Modality independent elastography (MIE): potential applications in dermoscopy. *Med Phys*. 2005;32(5):1308–20.
77. Miga MI. A new approach to elastography using mutual information and finite elements. *Phys Med Biol*. 2003;48(4):467–80.
78. Baldeusings RA, Danilouchkine MG, Mastik F, Schaar JA, Serruys PW, van der Steen AF. An inverse method for imaging the local elasticity of atherosclerotic coronary plaques. *IEEE Trans Inf Technol Biomed*. 2008;12(3):277–89.
79. Weiss S, Niederer P, Nava A, Caduff R, Bajka M. Inverse finite element characterization of the human myocardium derived from uniaxial compression experiments. *Biomed Tech (Berl)*. 2008;53(2):52–8.
80. Lopez O, Amrami KK, Manduca A, Rossman PJ, Ehman RL. Developments in dynamic MR elastography for in vitro biomechanical assessment of hyaline cartilage under high-frequency cyclical shear. *J Magn Reson Imaging*. 2007;25(2):310–20.
81. Guglielmi G, de Terlizzi F. Quantitative ultrasound in the assessment of osteoporosis. *Eur J Radiol*. 2009;71(3):425–31.
82. Vilayphiou N, Boutroy S, Sornay-Rendu E, van Rietbergen B, Munoz F, Delmas PD, et al. Finite element analysis performed on radius and tibia HR-pQCT images and fragility fractures at all sites in postmenopausal women. *Bone*. 2010; doi:10.1016/j.bone.2009.12.015.
83. Basford JR, Jenkyn TR, An KN, Ehman RL, Heers G, Kaufman KR. Evaluation of healthy and diseased muscle with magnetic resonance elastography. *Arch Phys Med Rehabil*. 2002;83(11):1530–6.
84. Chen Q, Basford J, An K-N. Ability of magnetic resonance elastography to assess taut bands. *Clin Biomech*. 2008;23(5):623–9.
85. Bensamoun SF, Ringleb SI, Chen Q, Ehman RL, An K-N, Brennan M. Thigh muscle stiffness assessed with magnetic resonance elastography in hyperthyroid patients before and after medical treatment. *J Magn Reson Imaging*. 2007;26(3):708–13.
86. Bensamoun SF, Ringleb SI, Littrell L, Chen Q, Brennan M, Ehman RL, et al. Determination of thigh muscle stiffness using magnetic resonance elastography. *J Magn Reson Imaging*. 2006;23(2):242–7.
87. Ringleb SI, Bensamoun SF, Chen Q, Manduca A, An KN, Ehman RL. Applications of magnetic resonance elastography to healthy and pathologic skeletal muscle. *J Magn Reson Imaging*. 2007;25(2):301–9.
88. Dombre ZJ, McCullough MB, Chen Q, An KN. Feasibility of using magnetic resonance elastography to study the effect of aging on shear modulus of skeletal muscle. *J Appl Biomech*. 2009;25(1):93–7.
89. Levinson SF, Shinagawa M, Sato T. Sonoelastic determination of human skeletal muscle elasticity. *J Biomech*. 1995;28(10):1145–54.
90. Hoyt K, Kneezel T, Castaneda B, Parker KJ. Quantitative sonoelastography for the in vivo assessment of skeletal muscle viscoelasticity. *Phys Med Biol*. 2008;53(15):4063–80.
91. Hoyt K, Castaneda B, Parker KJ. 5C-6 Muscle tissue characterization using quantitative sonoelastography: preliminary results. *ultrasonics symposium, 2007 IEEE*; 2007;365–8.
92. Hardy PA, Ridler AC, Chiarot CB, Plewes DB, Henkelman RM. Imaging articular cartilage under compression—cartilage elastography. *Magn Reson Med*. 2005;53(5):1065–73.
93. Neu CP, Hull ML, Walton JH, Buonocore MH. MRI-based technique for determining nonuniform deformations throughout the volume of articular cartilage explants. *Magn Reson Med*. 2005;53(2):321–8.
94. Lopez O, Amrami KK, Manduca A, Ehman RL. Characterization of the dynamic shear properties of hyaline cartilage using high-frequency dynamic MR elastography. *Magn Reson Med*. 2008;59(2):356–64.
95. Konofagou EE, Spalazzi JP, Lu HH. Elastographic imaging of the strain distribution at the anterior cruciate ligament and ACL-bone insertions. *Engineering in Medicine and Biology Society, 2005 IEEE-EMBS 2005 27th Annual International Conference*; 2005;972–5.
96. Farron J, Varghese T, Thelen DG. Measurement of tendon strain during muscle twitch contractions using ultrasound elastography. *IEEE Trans Ultrason Ferroelectr Freq Control*. 2009;56(1):27–35.
97. Klauser A, Peetrons P. Developments in musculoskeletal ultrasound and clinical applications. *Skeletal Radiol*. 2009; doi:10.1007/s00256-009-0782-y
98. Thitaikumar A, Righetti R, Krouskop TA, Ophir J. Resolution of axial shear strain elastography. *Phys Med Biol*. 2006;51(20):5245–57.
99. Othman SF, Xu H, Royston TJ, Magin RL. Microscopic magnetic resonance elastography (microMRE). *Magn Reson Med*. 2005;54(3):605–15.
100. Zysk AM, Nguyen FT, Oldenburg AL, Marks DL, Boppart SA. Optical coherence tomography: a review of clinical development from bench to bedside. *J Biomed Opt*. 2007;12(5):051403.